LIMNOLOGY and OCEANOGRAPHY

ASLO

Limnol. Oceanogr. 9999, 2023, 1–15

doi: 10.1002/lno.12350

Amino acid carbon isotope fingerprints are unique among eukaryotic microalgal taxonomic groups

Angela R. Stahl [1*] **Tatiana A. Rynearson** [1] **Kelton W. McMahon** [1]

Graduate School of Oceanography, University of Rhode Island, Narragansett, Rhode Island

Abstract

Eukaryotic microalgae play critical roles in the structure and function of marine food webs. The contribution of microalgae to food webs can be tracked using compound-specific isotope analysis of amino acids (CSIA-AA). Previous CSIA-AA studies have defined eukaryotic microalgae as a single functional group in food web mixing models, despite their vast taxonomic and ecological diversity. Using controlled cultures, this work characterizes the amino acid $\delta^{13}C$ ($\delta^{13}C_{AA}$) fingerprints—a multivariate metric of amino acid carbon isotope values—of four major groups of eukaryotic microalgae: diatoms, dinoflagellates, raphidophytes, and prasinophytes. We found excellent separation of essential amino acid $\delta^{13}C$ ($\delta^{13}C_{EAA}$) fingerprints among four microalgal groups (mean posterior probability reclassification of 99.2 ± 2.9%). We also quantified temperature effects, a primary driver of microalgal bulk carbon isotope variability, on the fidelity of $\delta^{13}C_{AA}$ fingerprints. A 10°C range in temperature conditions did not have significant impacts on variance in $\delta^{13}C_{AA}$ values or the diagnostic microalgal $\delta^{13}C_{EAA}$ fingerprints. These $\delta^{13}C_{EAA}$ fingerprints were used to identify primary producers at the base of food webs supporting consumers in two contrasting systems: (1) penguins feeding in a diatom-based food web and (2) mixotrophic corals receiving amino acids directly from autotrophic endosymbiotic dinoflagellates and indirectly from water column diatoms, prasinophytes, and cyanobacteria, likely via heterotrophic feeding on zooplankton. The increased taxonomic specificity of CSIA-AA fingerprints developed here will greatly improve future efforts to reconstruct the contribution of diverse eukaryotic microalgae to the sources and cycling of organic matter in food web dynamics and biogeochemical cycling studies.

Eukaryotic microalgae produce nearly half of the primary production on the planet (Field et al. 1998) and form the base of nearly all marine food webs (Falkowski et al. 2003; Not et al. 2012). The taxonomic composition of eukaryotic microalgae, in turn, impacts marine food web structure and function (Marrec et al. 2021), affecting the distribution and abundance of upper trophic level consumers, fisheries production, and the efficacy of the biological pump (Winder and Sommer 2012). For example, there are seasonal successions of microalgae in the Northwest Atlantic Ocean from diatom-fueled spring blooms supporting large bodied, lipid rich calanoid copepods to summer communities of dinoflagellates and picophytoplankton fed upon by small-bodied copepods. These seasonal successions have major implications for the foraging success of North Atlantic Right Whales (Sorochan et al. 2019) and the magnitude of regional export production (Stamieszkin et al. 2015). Furthermore, long-term regional changes in the microalgal community composition along the Western Antarctic Peninsula have been associated with observed changes in both krill (*Euphausia superba*) and penguin populations (Montes-Hugo et al. 2009). Developing analytical tools to reconstruct the links between microalgal taxa and upper trophic level consumers is a crucial, yet challenging task in food web ecology given the limitations of traditional observation, stomach content, and bulk stable isotope tools (Bartley et al. 2019).

To distinguish among broadly different taxonomic groups of primary producers and track their contribution to the flow of organic matter through food webs, researchers have used compound-specific isotope analysis of amino acids (CSIA-AA), a rapidly evolving approach that couples molecular-level biomarkers with stable isotope analyses (Close 2019). There is

*Correspondence: angela.stahl.r@gmail.com

Additional Supporting Information may be found in the online version of this article.

Present address: Department of Oceanography and Coastal Sciences, Louisiana State University, Baton Rouge, Louisiana

Author Contribution Statement: A.R.S., T.A.R. and K.W.M. designed the project. A.R.S. and K.W.M. performed laboratory analyses. A.R.S. analyzed the data. A.R.S. wrote the initial draft of the manuscript and A.R.S., T.A.R. and K.W.M. contributed to revisions of the manuscript.

tremendous diversity in the enzymatic synthesis pathways, carbon concentration mechanisms, and carbon fixation pathways that evolutionarily distinct primary producers use to make their amino acids (Hayes 2001; Scott et al. 2006). Taxon-specific biosynthetic processes have significant variations in carbon isotope dynamics (Hayes 2001; Scott et al. 2006; Bianchi and Canuel 2011; Besser et al. 2022), yielding distinct patterns or "fingerprints" when the $\delta^{13}C$ values of multiple amino acids ($\delta^{13}C_{AA}$) diagnostic of their primary producer sources are considered together (Scott et al. 2006; Larsen et al. 2009, 2013). Furthermore, the complex side chains of essential amino acids (EAA) typically cannot be de novo biosynthesized by most metazoans and must be directly acquired from diet with minimal isotopic discrimination (McMahon et al. 2010). Therefore, these unique $\delta^{13}C_{EAA}$ fingerprints among distinct primary producers are passed on to upper trophic level consumers virtually unmodified, acting as conservative tracers of primary producers supporting food webs (Elliot Smith et al. 2018; Rowe et al. 2019; Skinner et al. 2021).

Generally, the CSIA-AA approach has used multivariate coordinate space of EAAs (e.g., Thr, Ile, Val, Phe, and Leu), termed $\delta^{13}C_{EAA}$ fingerprints, to distinguish among broad taxonomic groups of primary producers, for example, among bacteria, fungi, terrestrial plants, and marine algae (Larsen et al. 2009, 2013). These broad taxonomic fingerprints have been used to reconstruct microalgae production in a coastal upwelling zone (Vokhshoori et al. 2014), examine grazing vs. detritivory in mangrove food webs (Harada et al. 2022), examine nutritional sources for facultative hindgut fermenting green sea turtles (Arthur et al. 2014), and characterize trophic niches of fish functional groups (Larsen et al. 2020). Recent work has exemplified the value of refining the taxonomic specificity of these $\delta^{13}C_{EAA}$ fingerprints, for example among different types of macroalgae to examine connectivity among nearshore habitats (Elliot Smith et al. 2018, 2022), among eukaryotic and prokaryotic microalgae to reconstruct millennial scale microalgal regime shifts (McMahon et al. 2015*a*), and among particulate organic matter (POM) and endosymbiotic algae in mixotrophic coral assemblages (Fox et al. 2019; Wall et al. 2021).

In most CSIA-AA studies to date, eukaryotic microalgae are often treated as one functional group despite having very different phylogenies, ecologies, and roles in biogeochemical cycling (Tirichine and Bowler 2011; Not et al. 2012). The extensive diversity among eukaryotic microalgae may underlie the large amount of otherwise unexplained variation in microalgal $\delta^{13}C_{EAA}$ data (Larsen et al. 2013; Rowe et al. 2019). We hypothesize that the significant variation in the current marine algae $\delta^{13}C_{EAA}$ fingerprints may in fact represent real, systematic variation among taxonomic groups of eukaryotic microalgae within this functionally grouped end member rather than simply noise about a mean. If true, characterization of different eukaryotic microalgal $\delta^{13}C_{EAA}$ fingerprints would have major implications for our ability to understand changing microalgal community dynamics and their impact on marine food webs, biogeochemical cycles, and fisheries and export production. To date, there have been no controlled, systematic experimental assessments of the diversity of $\delta^{13}C_{EAA}$ fingerprints among major taxonomic groups of eukaryotic microalgae, despite their ecological significance.

This study quantified eukaryotic microalgal $\delta^{13}C_{AA}$ fingerprints using controlled, laboratory microalgal cultures of four major groups of eukaryotic microalgae—diatoms (Class Bacillariophyceae), dinoflagellates (Class Dinophyceae), raphidophytes (Class Raphidophyceae), and prasinophytes (Class Mamiellophyceae) (Fig. S1). These four classes represent ecologically important groups of eukaryotic microalgae that span a large evolutionary diversity (Not et al. 2012). We included the raphidophytes, which come from the same Stramenopile lineage as diatoms, as an opportunity to test the separability of these more closely related microalgal lineages relative to the more distantly related prasinophytes and dinoflagellates. We hypothesized these different classes of microalgae would exhibit diagnostic $\delta^{13}C_{AA}$ fingerprints owing to evolutionary diversity in carbon fixation pathways and enzymatic steps of amino acid synthesis among different groups of primary producers (Larsen et al. 2013). We also explored the effect that temperature—a major driver of microalgal growth (Anderson et al. 2021) and bulk tissue $\delta^{13}C$ values (Rau et al. 1996; McMahon et al. 2013)—has on the fidelity of eukaryotic microalgal fingerprints. Previous work on broad taxonomic groups of primary producers suggests that taxonomically consistent $\delta^{13}C_{AA}$ fingerprints can be obtained despite variations in environmental and growth conditions by normalizing individual $\delta^{13}C_{AA}$ values (individual $\delta^{13}C_{AA}$ values minus the mean $\delta^{13}C_{AA}$ value of all amino acids in a sample) (Vokhshoori et al. 2014; Larsen et al. 2015; McMahon et al. 2016). We hypothesized that temperature would impact individual $\delta^{13}C_{AA}$ values, but not the relative offset among $\delta^{13}C_{AA}$ values within a species, such that normalization would maintain consistent, diagnostic $\delta^{13}C_{AA}$ fingerprints of different eukaryotic microalgae species across a 10°C range (15–25°C). To test the ability of eukaryotic microalgal $\delta^{13}C_{AA}$ fingerprints to track carbon flow to upper trophic level consumers, we applied our newly identified $\delta^{13}C_{AA}$ fingerprints to published consumer $\delta^{13}C_{AA}$ data in two contrasting systems: a polar system of penguins feeding on diatom-based krill (McMahon et al. 2015*b*) and a more complex mixotrophic system with corals supported by endosymbiotic dinoflagellate-production (Family Symbiodiniaceae; LaJeunesse et al. 2018) and water column eukaryotic microalgae through heterotrophic feeding on a mixed assemblage of POM and zooplankton (Fox et al. 2019). The improved specificity of eukaryotic microalgal $\delta^{13}C_{AA}$ fingerprints will open new doors for more refined studies of how changing microalgal community composition influences modern and paleo reconstructions of food web dynamics and biogeochemical cycling. Since this fingerprinting approach can be used on archival tissues, it alleviates some of the challenges of reconstructing paleo food web dynamics using

conventional techniques such as stomach contents, observations, or bulk stable isotope analysis, which requires preservation of baseline isotope data.

Methods

Culture conditions

To examine the diversity of $\delta^{13}C_{AA}$ fingerprints among eukaryotic microalgae, a library of three species from each of four major eukaryotic microalgae classes—diatoms (Class Bacillariophyceae), dinoflagellates (Class Dinophyceae), raphidophytes (Class Raphidophyceae), and prasinophytes (Class Mamiellophyceae)—was generated from established laboratory culture lines in the URI microalgal libraries and the National Center for Marine Algae and Microbiota (NCMA; formerly CCMP). Cultures were grown in triplicate under highly constrained growth conditions (Table S1). Cultures were grown in either f/2 or L1 media created using 0.22 μm filtered, autoclaved Narragansett Bay, Rhode Island seawater. All seawater was collected at the same time and location to ensure consistent water conditions for all cultures. Cultures were grown in climate-controlled incubators under 55 $\pm$ 10 μmol photons m-2 s-1 light intensity on a 12 h : 12 h light : dark cycle. To examine the impact of temperature on $\delta^{13}C_{AA}$ fingerprints, one species from each of the four groups, amenable to culture growth across the same temperature gradient, was grown in triplicate under three temperature treatments: 15°C, 20°C, and 25°C. Temperature treatments that produced maximum growth rate per species were determined from thermal tolerance data in published literature (Table S2).

A microplate reader (SpectraMax M5 Series, Molecular Devices) was used to obtain growth rates to target biomass collection approximately during exponential growth or early in the stationary phase. Once cultures reached sufficient density to obtain $\sim$ 5 mg of dry weight needed for CSIA-AA (culture density to dry weight relationship was determined from test cultures), cultures were gently vacuum filtered onto either 5 μm PETE membrane filters (Sterlitech), 2 μm PETE membrane filters (Sterlitech), or 0.22 μm PES membrane filters (Millipore Express PLUS) depending on the size of the species being filtered. Filtered biomass from each individual replicate culture was scraped from the filter, collected in precombusted (450°C for 6 h) glass vials, frozen at – 20°C, freeze dried for 72 h, homogenized with a spatula in the vial, and stored dry in vials until further analysis.

Compound-specific isotope analysis of amino acids

Approximately 5 mg of freeze-dried, homogenized samples were acid hydrolyzed in 0.5 mL of 6 N hydrochloric acid at 110°C for 20 h to isolate total free amino acids. Samples were then filtered through a 0.45 μm nylon syringe filter (Restek) and evaporated to dryness under a gentle stream of N_2. Five μL of nor-leucine (Sigma-Aldrich) with a known $\delta^{13}C$ value was added to each sample and standard as an internal calibration. Acid hydrolyzed samples were derivatized to N-trifluoroacetic acid isopropyl esters by esterification with acidified isopropanol followed by acylation with trifluoroacetic anhydride and dichloromethane to make amino acids amenable to gas chromatography (GC) (Silfer et al. 1991). The derivatized amino acids were redissolved in ethyl acetate and 1 μL was injected on column in splitless mode at 240°C. Individual amino acids were separated on a BPX5 column (60 m length, 0.32 mm ID, and 1 μm film thickness) in a Thermo Trace 1310 GC and analyzed on a Finnegan MAT Delta V Plus isotope ratio mass spectrometer (IRMS) interfaced to the GC through a GC-IsoLink II and reduction furnace (1000°C) at the University of Rhode Island, Graduate School of Oceanography. Standardization of runs was achieved using intermittent pulses of a CO_2 reference gas of known isotopic value.

To correct for the introduction of exogenous carbon and kinetic fractionation that occurred during derivatization, amino acid standards (Sigma-Aldrich) of known isotopic value—determined by individual analysis on an elemental analyzer-IRMS—were derivatized concurrently with samples and analyzed bracketing each sample. All samples were analyzed minimally in triplicate along with the amino acid mixed standard and a cyanobacteria working lab standard (Shen et al. 2021). Injections of the lab algal working standard were included in each batch run as a known-unknown for quality assurance and quality control purposes (Yarnes and Herszage 2017). The long-term reproducibility of $\delta^{13}C$ values in the lab algal standard was $\pm$ 0.7 ‰ (mean across all individual amino acids for > 50 separate full analyses), which provides an estimate of full protocol reproducibility (hydrolysis, wet chemistry, and isotope analysis).

We measured 13 individual amino acids with sufficient peak size and well-defined baseline chromatographic separation, which we classified as nonessential amino acids (NEAA) glycine (Gly), serine (Ser), alanine (Ala), aspartic acid/asparagine (Asx), glutamic acid/glutamine (Glx), proline (Pro) and EAA threonine (Thr), isoleucine (Ile), lysine (Lys), methionine (Met), valine (Val), phenylalanine (Phe), and leucine (Leu). Note, acid hydrolysis converts glutamine (Gln) and aspartamine (Asn) into Glu and Asp, respectively, due to cleavage of the terminal amine group, resulting in the measurement of combined Gln + Glu (referred to hereby as Glx), and Asn + Asp (referred to hereby as Asx). Stable isotope ratios are expressed relative to Vienna Pee Dee Belemnite in standard delta (δ) notation in per mil units (‰).

Statistical analyses

All statistical analyses were performed in R version 3.6.3 with RStudio interface version 1.1.456. Normalized $\delta^{13}C_{AAnorm}$ values were calculated using the following equation:

$$\delta^{13}C_{AAnorm} = \delta^{13}C_{AA} - \delta^{13}C_{AAmean} \quad (1)$$

where $\delta^{13}C_{AA}$ refers to the individual $\delta^{13}C_{AA}$ value that has been standard corrected for added exogenous carbon during

derivatization and $\delta^{13}C_{AAmean}$ refers to the mean of all $\delta^{13}C_{AA}$ values in a sample. The same equation was used when normalizing EAA $\delta^{13}C$ values, however, only the mean of all $\delta^{13}C_{EAA}$ values was used in this case. Here we used the five common EAA reported in CSIA-AA literature—Thr, Val, Leu, Ile, and Phe—since Lys can have coelution issues with tyrosine and Met is not abundant in many metazoans. We note that while these are the common EAA used in $\delta^{13}C_{EAA}$ fingerprinting, not all previous literature presenting primary producer $\delta^{13}C_{EAA}$ data use these amino acids, whether due to the derivatization procedures chosen, the GC running conditions used, or data selection choices post-analysis. This makes it challenging to compare broad libraries of $\delta^{13}C_{EAA}$ fingerprints across previously published studies and something important to consider in future studies to make published libraries more accessible to future applications.

We visually checked for departures from univariate normality on Q-Q plots. Differences in individual $\delta^{13}C_{AAnorm}$ values among the four microalgal classes were tested using multivariate ANOVA (MANOVA) combined with individual ANOVA pairwise comparisons and posthoc Tukey HSD test to evaluate the similarities and differences among groups for each amino acid. The null hypothesis that there was no difference in classification among the groups was tested by applying Pillai's trace with the MANOVA. Ward's hierarchical clustering (R-package Cluster; Maechler et al. 2022) and principal component analysis (PCA, R-package Vegan; Oksanen et al. 2013) were performed on $\delta^{13}C_{AAnorm}$ and $\delta^{13}C_{EAAnorm}$ values of eukaryotic microalgae to initially explore patterns and group memberships in the dataset. We used a linear discriminant function analysis (LDA; R package Modern Applied Statistics with S [MASS]; Venables and Ripley 2002) on our full suite of eukaryotic microalgal $\delta^{13}C_{AAnorm}$ values and $\delta^{13}C_{EAAnorm}$ values to examine combinations of independent variables (i.e., $\delta^{13}C_{AA}$ values) that best explained differences among the microalgal classes defined by the PCA and MANOVA. We used a leave-one-out cross-validation (R package caret) approach to calculate the probability of group membership.

We tested whether temperature had an impact on individual $\delta^{13}C_{AA}$ values and separation of both non-normalized and normalized $\delta^{13}C_{AA}$ fingerprints for a representative species within each microalgae group: diatoms (*Skeletonema marinoi*), dinoflagellates (*Prorocentrum micans*), raphidophytes (*Heterosigma akashiwo*), and prasinophytes (*Micromonas commoda*). First, we visually assessed patterns in variation among non-normalized and normalized individual $\delta^{13}C_{AA}$ values across temperature treatments: 15°C, 20°C, and 25°C. Among the four species, we looked for systematic variation in $\delta^{13}C_{AA}$ values among taxonomic groups and amino acid biosynthetic families as a function of temperature. To test our hypothesis that normalization reduces variation in $\delta^{13}C_{AA}$ values, we calculated the range in both $\delta^{13}C_{AA}$ values and $\delta^{13}C_{AAnorm}$ values across the three temperature treatments for each individual amino acid. We tested for differences between $\delta^{13}C_{AA}$ and $\delta^{13}C_{AAnorm}$ ranges using a Wilcoxon Rank Sum test for each amino acid corrected with a post-hoc Bonferroni test to limit a statistically significant result due to multiple tests. To examine the effect of temperature on the multivariate separation of eukaryotic microalgal $\delta^{13}C_{AA}$ fingerprints, we applied Ward's hierarchical clustering and PCA to $\delta^{13}C_{AA}$, $\delta^{13}C_{EAA}$, $\delta^{13}C_{AAnorm}$, and $\delta^{13}C_{EAAnorm}$ values of three replicate cultures per species per temperature treatment for one representative species from each of four groups of eukaryotic microalgae. We then used LDAs with a leave-one-out cross-validation approach to calculate the probability of group membership based on $\delta^{13}C_{AA}$, $\delta^{13}C_{EAA}$, $\delta^{13}C_{AAnorm}$, and $\delta^{13}C_{EAAnorm}$ values of three replicate cultures per species per temperature treatment for one representative species from each of four groups of eukaryotic microalgae.

We compared our eukaryotic microalgal $\delta^{13}C_{AA}$ data to previously published consumer data to test the ability of the $\delta^{13}C_{EAAnorm}$ fingerprints in this study to trace eukaryotic microalgal carbon sources to higher trophic consumers. First, we examined the primary producer carbon sources of gentoo penguins (*Pygoscelis papua*; McMahon et al. 2015*b*) using both the eukaryotic microalgal $\delta^{13}C_{EAAnorm}$ fingerprints from our study and macroalgal $\delta^{13}C_{EAAnorm}$ fingerprints from Larsen et al. (2013) to represent an additional endmember as these penguins are coastal foragers and have the potential to feed on invertebrates that obtain energy from nearshore benthic macroalgae (McMahon et al. 2015*b*). We used LDA and a leave-one-out cross-validation approach to predict group membership of penguins to primary producer source based on this compiled end member training data set. We used a similar approach to classify mixotrophic corals and their dinoflagellate endosymbionts (Symbiodiniaceae) (Fox et al. 2019) to our eukaryotic microalgal $\delta^{13}C_{EAAnorm}$ fingerprints supplemented with published cyanobacteria fingerprints (Lehman 2009; Larsen et al. 2013) to represent an additional water column primary producer, as well as heterotrophic bacterial fingerprints (Larsen et al. 2013) to represent a microbial detritus end member. We used LDA classification here to mirror the approach used by McMahon et al. (2015*b*) and Fox et al. (2019). While those studies identified the major contributing end members, they may be missing minor primary producer contributions, making it a challenge to accurately conduct a full mixing model approach. Thus, we felt the LDA was a more conservative approach to classification.

Results

Taxon-specific $\delta^{13}C_{AA}$ fingerprints

There was significant variation in individual $\delta^{13}C_{AA}$ values among the four eukaryotic microalgal groups (MANOVA, Pillai's trace = 2.81, $F_{39,123} = 46.6$, $p < 0.0001$; Fig. 1; Table S4). Twelve of the 13 amino acids measured had significant differences in $\delta^{13}C_{AA}$ values between at least two groups. Only the $\delta^{13}C_{AA}$ value of the EAA Val was not significantly

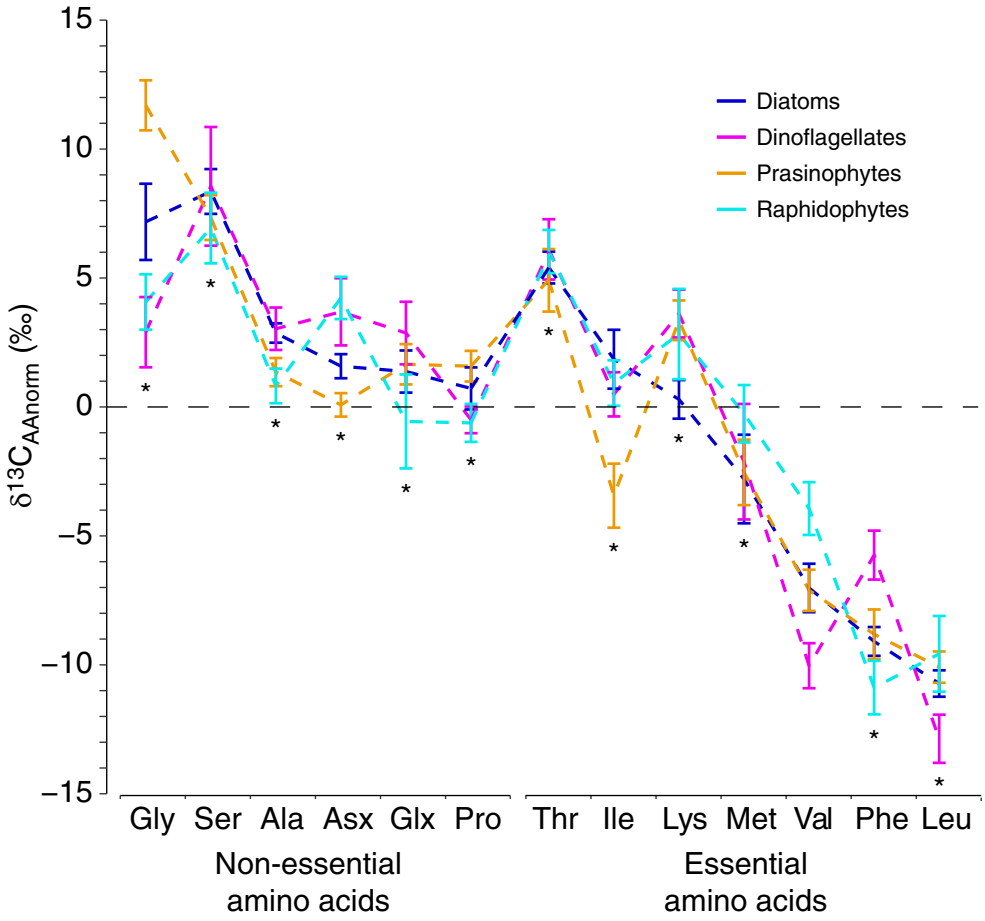

Fig. 1. Mean (± SD of three species per group) normalized individual amino acid $\delta^{13}C$ values ($\delta^{13}C_{AAnorm}$) of four groups of eukaryotic microalgae: diatoms (dark blue), dinoflagellates (magenta), prasinophytes (orange), and raphidophytes (cyan). Samples were grown at their ideal growth temperature. Amino acids were divided into nonessential and essential based on the ability of metazoans to synthesize, de novo, the carbon side chains. Asterisks signify significant differences among one or more groups within an individual amino acid (see Table S4). Dashed lines are to facilitate visualization of differences in relative patterns of $\delta^{13}C_{AAnorm}$ values among groups.

different among the four eukaryotic microalgal groups (Table S4). Patterns of $\delta^{13}C_{AA}$ values were similar for the three species within each taxonomic group, with the exception of outliers Glx and Lys in raphidophytes and Asx and Glx in dinoflagellates (Fig. S2). Rigorously testing isotope fingerprint separation at the species level was beyond the scope of this study's experimental design. The mean within group standard deviation in $\delta^{13}C_{AAnorm}$ values—calculated as the standard deviation in $\delta^{13}C_{AAnorm}$ values across three species within a group, averaged across all amino acids for all four groups—was 2.6 ± 1.0‰. The mean within group standard deviation was comparable for NEAA (2.6 ± 0.9‰) and EAA (2.6 ± 1.1‰).

Using PCA, which does not require a priori categorical variables, $\delta^{13}C_{AAnorm}$ fingerprints clustered in groups according to their phylogenetic association (Fig. 2a; Table S5). When all normalized amino acid $\delta^{13}C$ values were used, PC1 accounted for 32.3% of the variation and separated the diatoms, raphidophytes, and dinoflagellates. PC2 accounted for 26.2% of the variation and separated the prasinophytes and raphidophytes from the other two groups (Fig. 2a; Table S5). When the dataset was limited to only the normalized EAA commonly reported in CSIA-AA literature (Thr, Val, Leu, Ile, Phe), PC1 accounted for 55.6% of the variation and PC2 accounted for 25.4% of the variation, producing similar patterns of separation (Fig. 2b; Table S5).

Linear discriminant analysis using both $\delta^{13}C_{AAnorm}$ and $\delta^{13}C_{EAAnorm}$ values showed strong classification probability for the four taxonomic groups of microalgae (Fig. 3; Table S6). Among all the amino acids, the most important linear discriminants for separating the four categorical variables (eukaryotic microalgae) were the NEAA Asx and two EAA, Val, and Phe. When using the full suite of normalized amino acid $\delta^{13}C$ values, each group had a 100% posterior probability of being classified to its own group (Fig. 3a; Table S6) and ~ 93.3% of the variation was explained in the first two linear discriminants. When using the normalized EAA $\delta^{13}C$ values

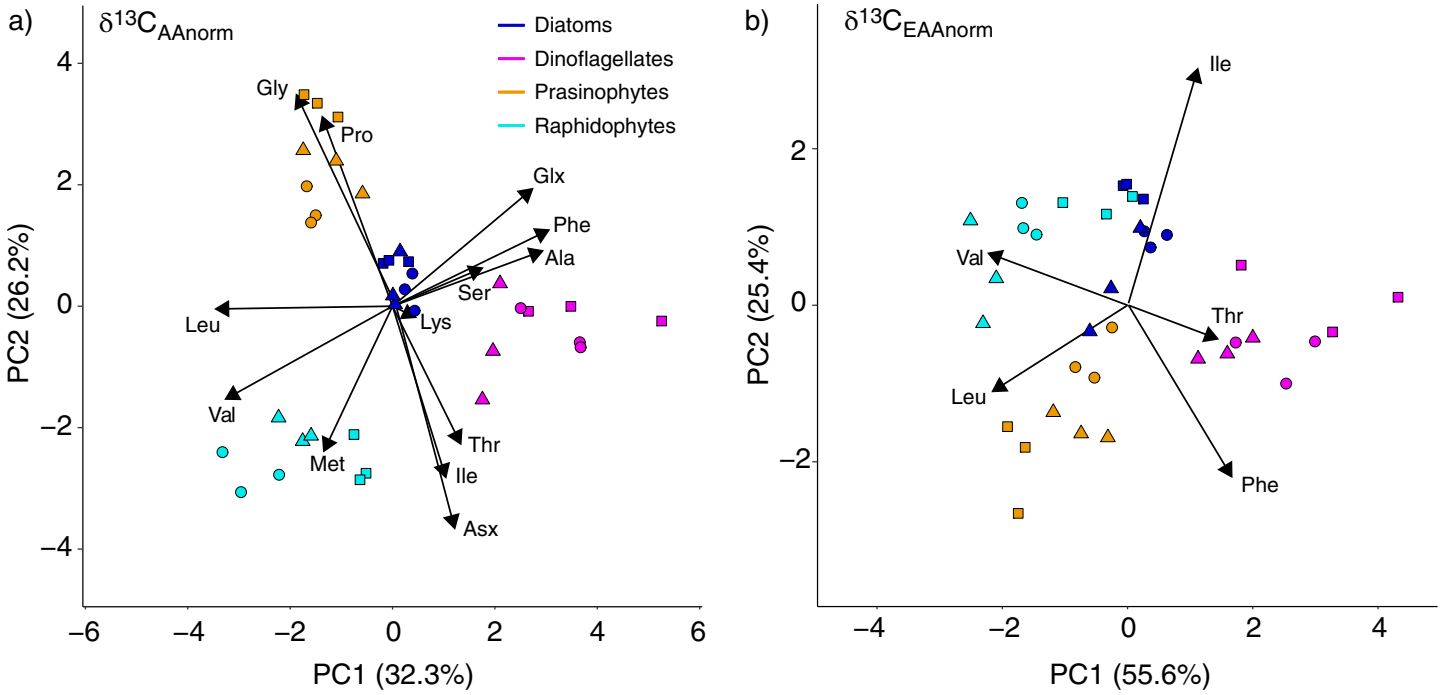

Fig. 2. Principal component analysis of (**a**) all 13 measured normalized individual amino acid $\delta^{13}C$ values ($\delta^{13}C_{AAnorm}$) and (**b**) five normalized essential amino acid $\delta^{13}C$ values ($\delta^{13}C_{EAAnorm}$) (Thr, Ile, Val, Phe, and Leu) for three replicate cultures of three species each of four different groups of eukaryotic microalgae: diatoms: *Chaetoceros debilis* (dark blue square), *Skeletonema marinoi* (dark blue circle), and *Thalassiosira rotula* (dark blue triangle); dinoflagellates: *Akashiwo sanguinea* (magenta squares), *Prorocentrum micans* (magenta circles), *Heterocapsa triquetra* (magenta triangles); prasinophytes: *Micromonas pusilla* (orange squares), *Micromonas commoda* (orange circles), *Ostreococcus lucimarinus* (orange triangles); and raphidophytes: *Fibrocapsa japonica* (cyan squares), *Heterosigma akashiwo* (cyan circles), *Viridilobus marinus* (cyan triangles). Cultures were grown at their ideal growth temperatures. Percent variance explained by each principal component is in parentheses on each axis. Loadings for individual amino acids are represented as arrows from the origin.

(Thr, Val, Leu, Ile, and Phe), eight of nine diatom samples (88.9%) were correctly classified with 97.9 ± 6.0% posterior probability and one diatom sample (*T. rotula*) was classified as a prasinophyte with 78.7% probability (Fig. 3b; Table S6). All dinoflagellates (99.9 ± 0.2% probability), prasinophytes (99.9 ± 1.7%), and raphidophytes (99.8 ± 0.3%) were correctly classified and 98.1% of the total variation was explained in the first two linear discriminants (Fig. 3b; Table S6).

Thermal effects on taxon-specific $\delta^{13}C_{AA}$ fingerprints

$\delta^{13}C_{AA}$ values varied among temperature treatments, though the patterns in variation were not consistent across amino acids, species, or amino acid biosynthetic families (Fig. S3). For example, $\delta^{13}C_{NEAA}$ values in the dinoflagellate *P. micans* were lower at 15°C than at 20°C or 25°C, but not in any other species examined. Similarly, $\delta^{13}C_{EAA}$ values were lower in the 15°C temperature treatment for the diatom *S. marinoi* and raphidophyte *H. akashiwo* (Fig. S3) but not in the other species. The prasinophyte *M. commoda* showed no consistent patterns in $\delta^{13}C_{AA}$ values among temperature treatments. Normalization of amino acids reduced the small amount of variation across temperature treatments, with some notable outliers, for example, Ile in the prasinophyte and raphidophyte (Fig. S3).

Normalization of $\delta^{13}C_{AA}$ values across temperature treatments reduced variance in $\delta^{13}C$ values across temperature treatments relative to non-normalized amino acids (Fig. S4). Patterns were generally consistent across species: 2.3 ± 0.8‰ (normalized) vs. 2.6 ± 0.7‰ (non-normalized) for the diatom *S. marinoi*, 2.9 ± 0.9‰ (normalized) vs. 5.3 ± 1.7‰ (non-normalized) for the dinoflagellate *P. micans*, 3.0 ± 0.8‰ (normalized) vs. 3.9 ± 0.9‰ (non-normalized) for the raphidophyte *H. akashiwo*, and 3.0 ± 0.8‰ (normalized) vs. 4.0 ± 1.0‰ (non-normalized) for the prasinophyte *M. commoda* (Fig. S4). However, a Bonferroni corrected Wilcoxon rank sum test showed no significant difference ($p > 0.05$) between normalized and non-normalized $\delta^{13}C_{AA}$ range due to temperature for each amino acid.

$\delta^{13}C_{AA}$ fingerprints maintained their taxonomic clustering even with the moderate temperature-induced variation in individual $\delta^{13}C_{AA}$ values (Fig. 4; Table S7). With ($\delta^{13}C_{AAnorm}$ values, Fig. 4b) and without normalization ($\delta^{13}C_{AA}$ values, Fig. 4a), replicate cultures at different temperature treatments clustered according to their taxonomic association. Normalized ($\delta^{13}C_{EAAnorm}$ values, Fig. 4d) and non-normalized

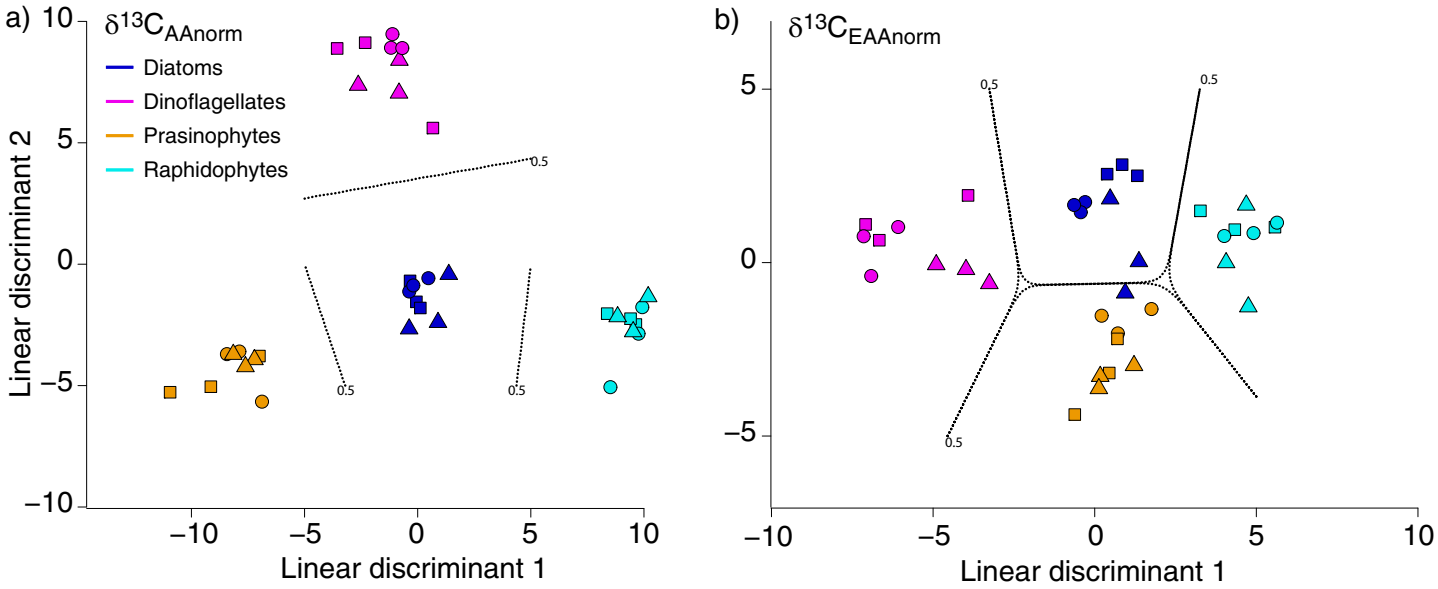

Fig. 3. Linear discriminant function analysis of (**a**) all 13 measured normalized individual amino acid $\delta^{13}C$ values ($\delta^{13}C_{AAnorm}$) and (**b**) five normalized EAA $\delta^{13}C$ values ($\delta^{13}C_{EAAnorm}$) (Thr, Ile, Val, Phe, and Leu) for three replicate cultures of three species each of four different groups of eukaryotic microalgae: Diatoms: *Chaetoceros debilis* (dark blue square), *Skeletonema marinoi* (dark blue circle), *Thalassiosira rotula* (dark blue triangle); Dinoflagellates: *Akashiwo sanguinea* (magenta squares), *Prorocentrum micans* (magenta circles), *Heterocapsa triquetra* (magenta triangles); Prasinophytes: *Micromonas pusilla* (orange squares), *Micromonas commoda* (orange circles), *Ostreococcus lucimarinus* (orange triangles); and Raphidophytes: *Fibrocapsa japonica* (cyan squares), *Heterosigma akashiwo* (cyan circles), *Viridilobus marinus* (cyan triangles). Samples were grown at their ideal growing temperature. The dotted lines represent confidence ranges at $p = 0.5$.

($\delta^{13}C_{EAA}$ values, Fig. 4c) EAA accounted for more of the total variability in the first two principal components when compared to all amino acids. Even without normalization, all samples across the three temperature treatments were classified correctly to their own taxonomic group with 99.9% posterior probability based on all $\delta^{13}C_{AA}$ values (Fig. 5a; Table S8) and only $\delta^{13}C_{EAA}$ values (Thr, Ile, Val, Phe, and Leu) (Fig. 5b; Table S8). The most important EAA for separating the taxonomic groups in the temperature experiment were Phe and Leu (Table S8), which were the amino acids that were important for separating the taxonomic groups in the broader diversity assessment as well (Fig. 3). After normalization, all diatoms, dinoflagellates, prasinophytes, and raphidophytes were correctly classified to their own group with 99.9% posterior probability or greater based on their $\delta^{13}C_{AAnorm}$ values (Fig. 5b; Table S8) and $\delta^{13}C_{EAAnorm}$ values (Fig. 5d; Table S8).

Applications to upper trophic level consumers

We applied $\delta^{13}C_{EAAnorm}$ fingerprints of eukaryotic microalgae from this study to two published consumer $\delta^{13}C_{EAAnorm}$ datasets to examine the common application of identifying primary producer carbon sources of food webs supporting higher trophic level consumers. In the case study of adult gentoo penguins in the Antarctic Peninsula (McMahon et al. 2015*b*), we generated a primary producer LDA model that included both our microalgal-derived $\delta^{13}C_{EAAnorm}$ values and previously published macroalgal $\delta^{13}C_{EAAnorm}$ values (Larsen et al. 2013). This model accurately classified all of the dinoflagellates, prasinophytes, and raphidophytes to their taxonomic classification with $98.0 \pm 6.9\%$, $94.1 \pm 13.4\%$ and $97.9 \pm 4.7\%$ posterior probability, respectively. The model accurately classified 14 out of 15 (93.3%) diatom samples with $96.7 \pm 11.0\%$ probability and 15 out of 16 (93.8%) macroalgal samples with $99.7 \pm 0.9\%$ probability (Fig. 6a; Table S9) to their taxonomic classification. Adding gentoo penguin $\delta^{13}C$ data to this model showed four out of five penguin (80%) $\delta^{13}C_{EAAnorm}$ patterns had an $86.1 \pm 21.3\%$ posterior probability that the source of their EAA most closely resembled the diatom $\delta^{13}C_{EAAnorm}$ fingerprint with one penguin $\delta^{13}C_{EAAnorm}$ pattern resembling the dinoflagellate $\delta^{13}C_{EAAnorm}$ fingerprint with a 97.8% posterior probability (Fig. 6a; Table S9).

To identify primary producers supporting the food webs of mixotrophic corals (Fox et al. 2019), we first generated a primary producer LDA model that included our microalgal-derived $\delta^{13}C_{EAAnorm}$ values in addition to previously published cyanobacteria (Lehman 2009; Larsen et al. 2013) and heterotrophic bacteria (Lehman 2009; Larsen et al. 2013) $\delta^{13}C_{EAAnorm}$ values. This model accurately classified 100% of bacteria ($99.7 \pm 1.2\%$ posterior probability), dinoflagellates ($97.1 \pm 3.9\%$ posterior probability), raphidophytes ($92.0 \pm 11.1\%$ posterior probability), and prasinophytes ($86.3 \pm 14.7\%$ posterior probability) to their taxonomic classification. The model also accurately classified six out of 10 (60%) cyanobacteria with $96.2 \pm 6.0\%$ posterior probability

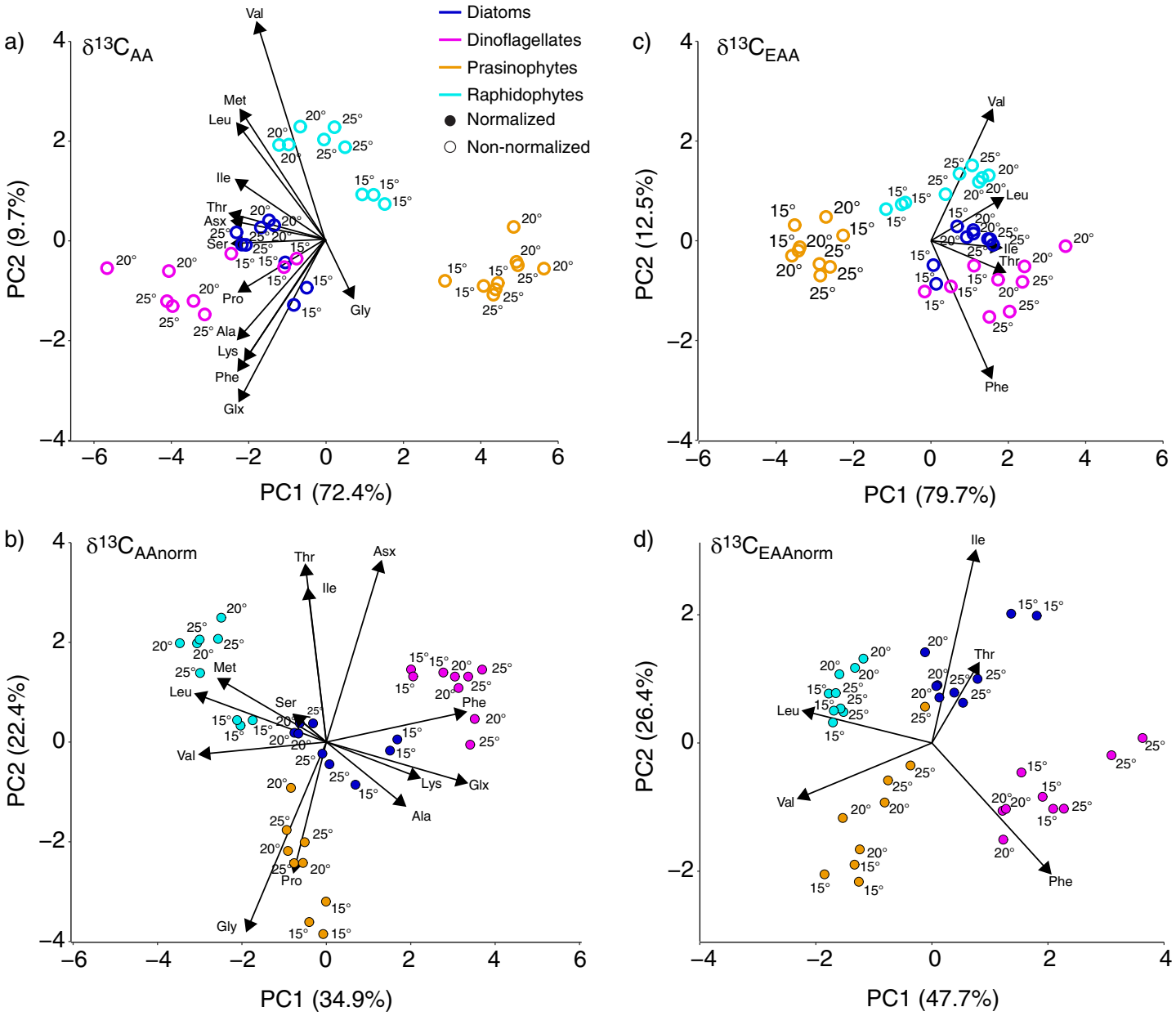

Fig. 4. Principal component analysis of (**a**) all 13 measured amino acid $\delta^{13}C$ values ($\delta^{13}C_{AA}$), (**b**) all 13 measured normalized individual amino acid $\delta^{13}C$ values ($\delta^{13}C_{AAnorm}$), (**c**) five EAA (Thr, Ile, Val, Phe, and Leu) $\delta^{13}C$ values ($\delta^{13}C_{EAA}$), and (**d**) five normalized EAA $\delta^{13}C$ values ($\delta^{13}C_{EAAnorm}$) of four eukaryotic microalgal species: diatoms *Skeletonema marinoi* (dark blue), dinoflagellates *Prorocentrum micans* (magenta), prasinophytes *Micromonas commoda* (orange), and raphidophytes *Heterosigma akashiwo* (cyan) grown at three temperature treatments 15°C, 20°C, and 25°C (three replicate cultures per group per temperature treatment). Percent variance explained by each principal component is in parentheses on each axis. Loadings for individual amino acids are represented as arrows from the origin.

and 14 out of 15 diatoms (93.3%) with 92.3 ± 13.9% posterior probability (Fig. 6b, Table S9) to their taxonomic classification. When coral-extracted Symbiodiniaceae $\delta^{13}C_{EAAnorm}$ were added to this model, eight out of 11 Symbiodiniaceae (72.7%) were classified as dinoflagellates with 89.3 ± 9.6% probability and three out of 11 Symbiodiniaceae (27.3%) were classified as diatoms with 75.6 ± 7.4% probability. Using this model to reveal coral EAA sources, our LDA showed seven out of 19 coral samples (36.8%) had an 80.0 ± 16.3% posterior probability that they received their EAA from dinoflagellates, six out of 19 coral samples (31.6%) had a 62.3 ± 22.8% posterior probability their EAA source was prasinophytes, five out of 19 coral samples (26.3%) had an 80.4 ± 10.2% posterior probability of a diatom EAA source, and one out of 19 corals (5.2%) had an 74.7% posterior probability that their EAA source was cyanobacteria (Fig. 6b; Table S9).

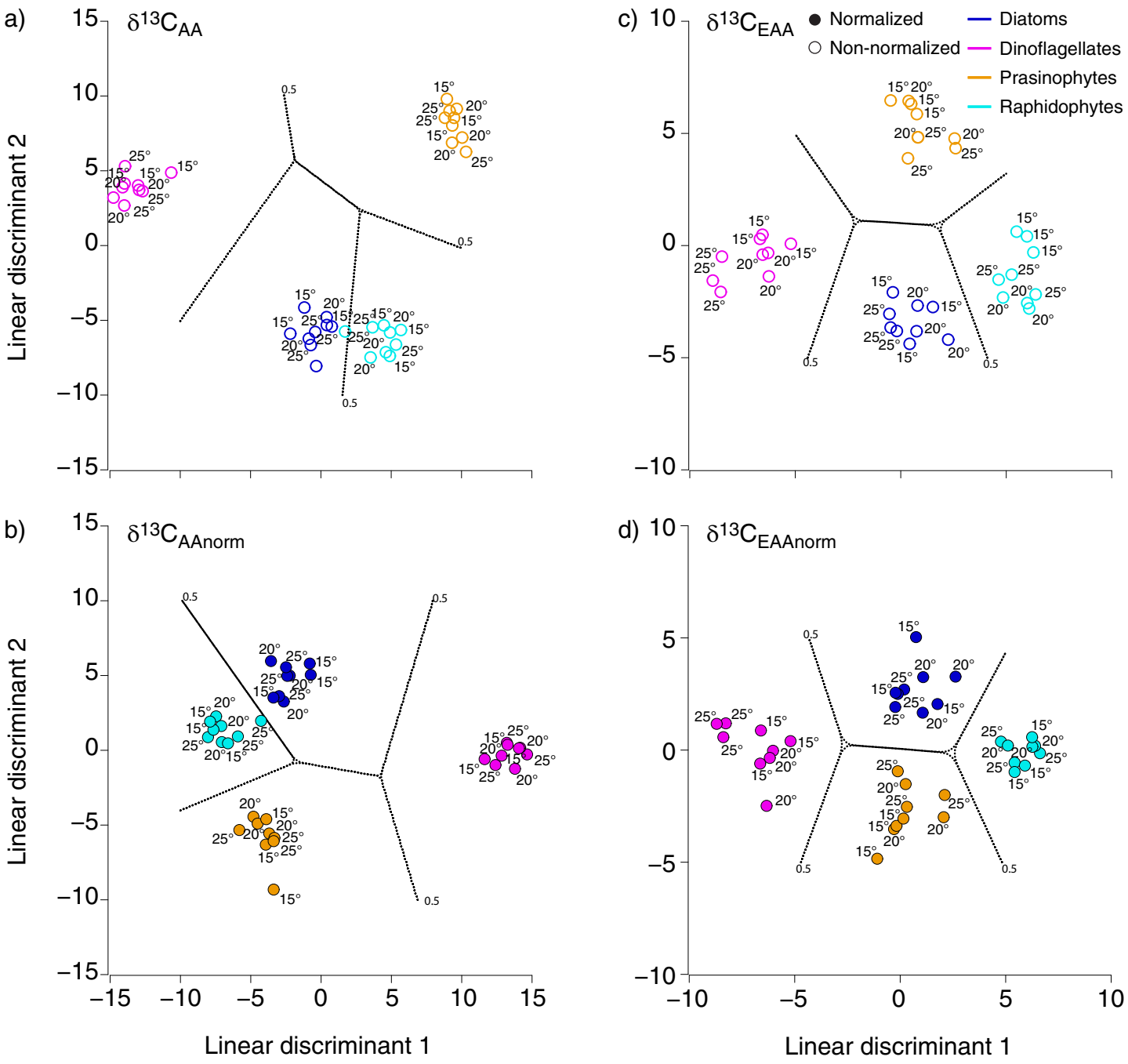

Fig. 5. Linear discriminant function analysis based of (**a**) all 13 measured amino acid $\delta^{13}C$ values ($\delta^{13}C_{AA}$), (**b**) all 13 measured normalized individual amino acid $\delta^{13}C$ values ($\delta^{13}C_{AAnorm}$), (**c**) five EAA (Thr, Ile, Val, Phe, Leu) $\delta^{13}C$ values ($\delta^{13}C_{EAA}$), and (**d**) five normalized EAA $\delta^{13}C$ values ($\delta^{13}C_{EAAnorm}$) of four eukaryotic microalgal species: diatoms *Skeletonema marinoi* (dark blue), dinoflagellates *Prorocentrum micans* (magenta), prasinophytes *Micromonas commoda* (orange), and raphidophytes *Heterosigma akashiwo* (cyan) grown at three temperature treatments 15°C, 20°C, and 25°C (three replicate cultures per group per temperature treatment). Dotted lines represent confidence ranges at $p = 0.5$.

Discussion

Taxon-specific $\delta^{13}C_{AA}$ fingerprints

CSIA-AA is quickly emerging as a powerful tool to identify distinct primary producer sources and track their relative contribution of carbon to upper trophic level consumers (Close 2019). Yet, the taxonomic resolution of these fingerprints is still not well constrained, particularly among eukaryotic microalgae that play key roles in global ocean food webs,

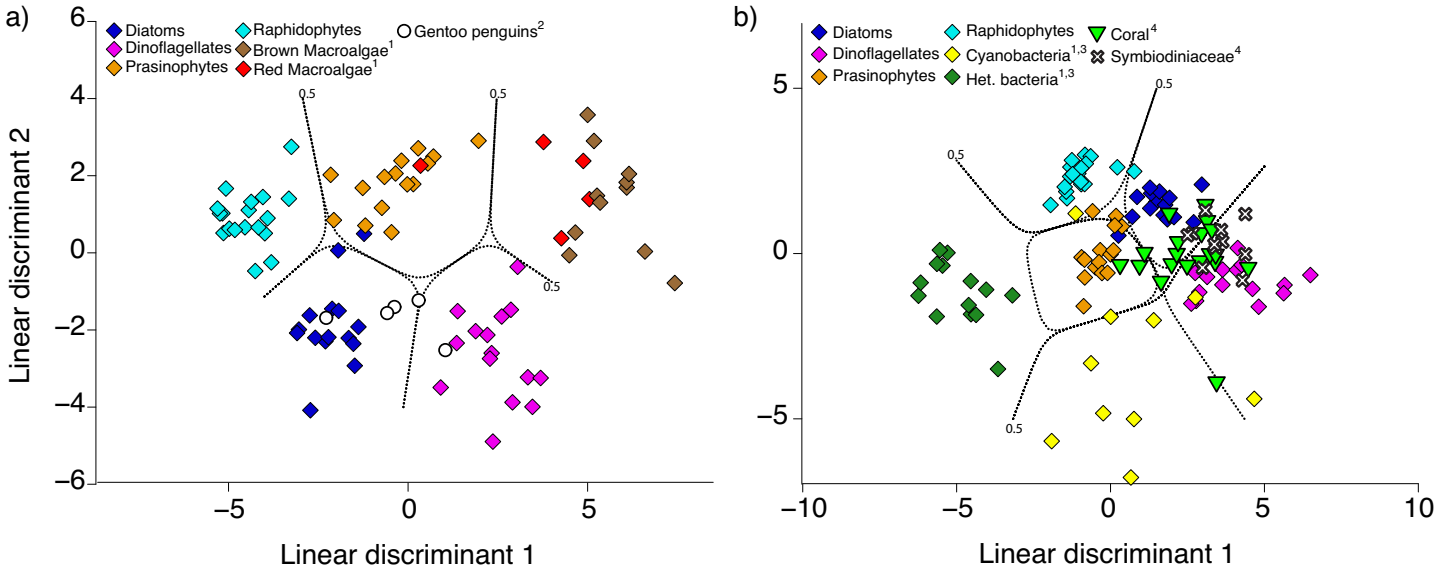

Fig. 6. Linear discriminant function analysis of end member and consumer normalized EAA $\delta^{13}C$ values (Thr, Ile, Val, Phe, and Leu) ($\delta^{13}C_{EAAnorm}$) values from two contrasting systems. (**a**) gentoo penguins $\delta^{13}C_{EAAnorm}$ values (open circles, *Pygoscelis papua*, [2]McMahon et al. 2015*b*) and end members: diatoms (dark blue diamonds), dinoflagellates (magenta diamonds), prasinophytes (orange diamonds), and raphidophytes (cyan diamonds) from this study and red macroalgae (red diamonds) and brown macroalgae (brown diamonds) from [1]Larsen et al. 2013. (**b**) mixotrophic corals $\delta^{13}C_{EAAnorm}$ values (green inverted triangles, *Pocillopora meandrina*, [4]Fox et al. 2019), Symbiodiniaceae (open Xs, [4]Fox et al. 2019), and end members of diatoms, dinoflagellates, prasinophytes, and raphidophytes from this study and cyanobacteria (yellow diamonds, [1]Larsen et al. 2013; [3]Lehman 2009) and heterotrophic bacteria (olive diamonds, [1]Larsen et al. 2013; [3]Lehman 2009). Dotted lines represent confidence ranges at $p = 0.5$.

biogeochemical cycles, and the biological pump. Here, we find clear separation in multivariate $\delta^{13}C_{AAnorm}$ and $\delta^{13}C_{EAAnorm}$ space among four major groups of eukaryotic microalgae—diatoms, dinoflagellates, raphidophytes, and prasinophytes—that were previously grouped together into one "microalgae" category in CSIA-AA mixing models (Larsen et al. 2013; McMahon et al. 2015*a*,*b*, 2016; Rowe et al. 2019). Diatoms clustered more closely with raphidophytes than dinoflagellates or prasinophytes in PCA space based on $\delta^{13}C_{AAnorm}$ values (Fig. 2), which makes sense evolutionarily as diatoms and raphidophytes are both part of the Heterokont/Stramenopile lineage, while dinoflagellates are part of the Alveolate lineage, and prasinophytes come from the Chlorophyte lineage (Not et al. 2012) (Fig. S1). The amino acids Leu, Val, and Phe were important for separating diatoms, raphidophytes, and dinoflagellates, whereas Asx, Ile, Pro, and Gly were important for separating the prasinophytes and raphidophytes from the other groups (Table S5). In previous literature, Leu and Val were also found to be some of the most important amino acids for separating broader taxonomic groups of algae, bacteria, fungi, and terrestrial plants (Larsen et al. 2013).

Evolutionary divergence is thought to be the driving force behind the unique biosynthesis pathways primary producers use to make their amino acids and therefore the unique $\delta^{13}C_{AAnorm}$ fingerprints we observe among taxonomic groups. The prevailing evidence supports the theory that metabolic pathway evolution followed the patchwork assembly model (Ycas 1974; Jensen 1976) where ancestral enzymes were generalists and therefore could react with a wide range of related substrates to carry out the same type of reaction. Subsequent gene duplication, fusion or elongation resulted in enzymes with high affinity and specificity for a substrate, which led to the diversification of function, expansion of metabolic capabilities, and development of new pathways (Lazcano et al. 1992; Fani and Fondi 2009). This model of metabolic pathway evolution would particularly affect EAA, which have many more independent enzymatic steps in their synthesis pathways than NEAA, leading to multiple opportunities for isotopic branch points that create unique producer $\delta^{13}C_{AAnorm}$ fingerprints (Hayes 2001). For example, Leu belongs to the group of neutral-polar amino acids that includes Gly, Val, and Ile, and its biosynthesis involves a five-step conversion process starting with the Val precursor 3-methyl-2-oxobutanoate (Binder 2010). Similarly, Ile biosynthesis requires 11 reaction steps, and the last four steps also carry out reactions involved in Val and Leu biosynthesis (Kohlmeier 2003). While much is known about the evolution of amino acid biosynthetic pathways, future work should be aimed at studying the isotope effects associated with divergent amino acid synthesis pathways, carbon concentration mechanisms, or carbon fixation pathways among closely related taxa to allow for better a priori predictions of likely taxonomic separation of primary producer $\delta^{13}C_{AA}$ fingerprints from a first principles perspective.

In our study, using all amino acid $\delta^{13}C$ values produced better separation of eukaryotic microalgal group fingerprints than focusing on EAA $\delta^{13}C$ values alone. Thus, in applications without risk of trophic modification, for example in characterizing microalgal community composition in the absence of consumers, using the full suite of normalized amino acid $\delta^{13}C$ values will better aid taxonomic separation. However, the most common applications of CSIA-AA fingerprinting involve consumers and associated trophic modification that can alter NEAA $\delta^{13}C$ values in, as of yet, poorly constrained ways (McMahon et al. 2010, 2015*b*; Newsome et al. 2011), obscuring the original primary producer fingerprint. In these situations, it is important to use EAA $\delta^{13}C$ values that are directly incorporated into consumer tissues with little trophic discrimination (McMahon et al. 2010; Newsome et al. 2011; Takizawa et al. 2020). In this study, when only using normalized EAA $\delta^{13}C$ values (i.e., the approach with the least discriminatory power), there was still excellent separation among the four taxonomic groups of eukaryotic microalgae with accurate reclassification rates of 99.2 ± 3.0%. This finding is critical to using these high taxonomic resolution eukaryotic microalgal $\delta^{13}C_{EAAnorm}$ fingerprints as reliable tracers for carbon sources throughout marine food webs.

Thermal effects on taxon-specific $\delta^{13}C_{AA}$ fingerprints

It is often not feasible for consumer resource utilization studies using CSIA-AA fingerprinting to collect and characterize local producers at the time of consumer foraging, particularly when studying highly migratory species or paleosystems. As such, studies often use literature data on $\delta^{13}C_{EAA}$ fingerprints from natural and cultured primary producer collections to characterize resource utilization patterns of consumers across a wide range of systems. This approach relies on the assumption that normalized $\delta^{13}C_{EAA}$ fingerprints are robust to changing environmental conditions (e.g., Arthur et al. 2014; MacDonald et al. 2019; Phillips et al. 2020). One of the only studies to rigorously test this concept was Larsen et al. (2015), who found that normalizing $\delta^{13}C_{AA}$ values to their mean in a marine diatom species (*Thalassiosira weissflogii*) cultured across a range of light, salinity, temperature, and pH conditions significantly reduced $\delta^{13}C_{AA}$ variance. They concluded that while differing oceanic growth conditions can change individual $\delta^{13}C_{AA}$ values, the $\delta^{13}C_{AA}$ fingerprints remain largely invariant. From this experiment, we hypothesized that temperature would be the primary driver of microalgal $\delta^{13}C_{AA}$ variation, as it is one of the major determinants of microalgal growth rate (Anderson et al. 2021) and geographic variation in microalgal bulk $\delta^{13}C$ values (Rau et al. 1989, 1996). While we did observe a reduction in $\delta^{13}C_{AA}$ range following the normalization process, LDA reclassification probabilities to the correct taxonomic group were high with and without normalization, indicating that the $\delta^{13}C_{AA}$ fingerprints were not highly sensitive to temperature conditions. This work reinforces the growing body of literature indicating that $\delta^{13}C_{AA}$ fingerprints stem from the evolutionary diversity of the amino acid synthesis pathways and are robust to environmental or geographic influences.

Within species, we observed thermally dependent separation of $\delta^{13}C_{AAnorm}$ fingerprints that were likely associated with kinetic isotope effects that are evident even after normalization (DeNiro and Epstein 1977). It is tempting to speculate about the fine scale separation of fingerprints with temperature, but the variance at this resolution is likely too small to be ecologically relevant in field applications. The effects of temperature were also apparent on individual $\delta^{13}C_{AA}$ values, for example, in the $\delta^{13}C_{EAA}$ values in the diatom, *S. marinoi*, and raphidophyte, *H. akashiwo*, as well as the $\delta^{13}C_{NEAA}$ values in the dinoflagellate, *P. micans*. NEAA isotope fractionation is an underexplored area of CSIA-AA research, but some studies have attempted to develop quantitative metrics of growth condition using $\delta^{13}C_{AA}$ data (Newsome et al. 2014; McMahon et al. 2015*b*; Whiteman et al. 2018; Fry and Carter 2019). However, we did not observe any consistent patterns in temperature-induced variation on individual $\delta^{13}C_{AA}$ values across species, amino acid biosynthetic families, or temperature treatments. Future work is warranted to systematically explore the impacts of a wider range of environmental conditions—such as nutrient concentrations, irradiance, salinity or > 10°C ranges in temperature—on $\delta^{13}C_{AA}$ absolute values across a much broader taxonomic range of species and their diversity of metabolic and growth capacities.

Applications to upper trophic level consumers

We applied the newly identified $\delta^{13}C_{EAAnorm}$ fingerprints to trace the primary microalgal EAA source contribution using published $\delta^{13}C_{EAA}$ data from consumers representing two distinct food webs—a simple diatom-based polar food chain (McMahon et al. 2015*b*) and a more complex tropical coral mixotrophic system (Fox et al. 2019). Microalgae were identified as the dominant source of EAA supporting wild adult gentoo penguins (*Pygoscelis papua*) from King George Island, Antarctica using broad taxonomic $\delta^{13}C_{EAA}$ fingerprints (McMahon et al. 2015*b*) but could not infer any finer scale detail on the types of eukaryotic microalgae supporting the penguin food web. Our model using finer taxonomic resolution microalgal fingerprints indicates diatoms as the key base of these gentoo penguins' food web. This finding matches expectations as penguins in this area have been shown to feed on krill that forage preferentially on diatoms (e.g., Ducklow et al. 2007). Identifying the specific types of microalgae supporting polar food webs has important implications for predicting food chain length (Barnes et al. 2010), which can affect the amount of energy available to upper trophic level consumers with major implications for the ecological trajectories of these communities (Ward and McCann 2017). For example, recent changes in environmental conditions in the western Antarctic peninsula caused a southward shift of large microalgal cells (mainly diatoms), which in turn caused a

cascading reorganization of the food web supported by diatoms (Montes-Hugo et al. 2009). Going forward, our newly developed suite of eukaryotic microalgal $\delta^{13}C_{EAAnorm}$ fingerprints will provide a quantifiable tool to link the impacts of microalgal community composition on changing trophic dynamics and food web structure.

Mixotrophic corals offer a second, more complex case study to test the application of our eukaryotic microalgal $\delta^{13}C_{EAAnorm}$ fingerprints and tease apart microalgae EAA contributions to consumers. Corals are mixotrophic consumers that obtain organic carbon autotrophic photosynthate from endosymbiotic dinoflagellates (Symbiodiniaceae) as well as from water column primary production (e.g., eukaryotic microalgae, cyanobacteria, and heterotrophic bacteria) via heterotrophic feeding on zooplankton (Ferrier-Pagès et al. 2011). The $\delta^{13}C_{EAA}$ fingerprints of these various primary producers are passed up the food chain via heterotrophic feeding virtually unmodified and recorded in the tissues of coral consumers. In a study looking at the contributions of autotropy vs. heterotrophy, cauliflower corals (*Pocillopora meandrina*) on Palmyra Atoll in the Pacific Ocean Northern Line Islands were found to obtain the majority of their amino acids from autotrophy and the rest from the broad water column community of zooplankton, microalgae, POM, and bacteria via heterotrophic feeding (Fox et al. 2019). We applied our fine-scale eukaryotic microalgal $\delta^{13}C_{EAAnorm}$ fingerprints to these published *P. meandrina* and the dinoflagellate endosymbionts isolated from those corals to better constrain carbon sources supporting this mixotrophic assemblage via trophic transfer. We found that the majority of dinoflagellate endosymbionts (72.7%) classified as dinoflagellates, as expected for symbionts in the family Symbiodiniaceae. This result is compelling given that field collected dinoflagellates from the published literature, cultured dinoflagellates from this study, and dinoflagellate endosymbionts isolated from wild corals all classified with our dinoflagellate $\delta^{13}C_{EAAnorm}$ fingerprints. These findings support data from Wall et al. (2021), who also found distinct differences among $\delta^{13}C_{EAAnorm}$ fingerprints between heterotrophic production sources (POM, plankton, and microalgae) and endosymbiotic Symbiodiniaceae in controlled feeding studies, showing that *Montipora capitata* corals aligned with Symbiodiniaceae while *Pocillopora meandrina* spanned a continuum between autotrophic Symbiodiniaceae and heterotrophy. These patterns of strong separation between water column eukaryotic microalgae and endosymbiotic dinoflagellates within corals may reflect some evolutionary differences in Symbiodiniaceae associated with the symbiotic lifecycle (Ros et al. 2020). Our data also support the conclusions of previous amino acid isotope fingerprinting studies that found corals fell along a continuum between autotrophy (endosymbiotic dinoflagellates) and heterotrophy (other microalgae consumed via zooplankton) (e.g., Fox et al. 2019; Wall et al. 2021).

For the 27% of Symbiodiniaceae that were incorrectly classified as diatoms, it is interesting to note that this has been observed in other endmember fingerprinting data as well. For example, several of the cyanobacteria from Larsen et al. 2013 classify as either dinoflagellates, prasinophytes, or raphidophytes. This may be a function of the subset of EAA we chose to examine in our LDA to maximize separation across all groups or it may be an indication of approaching the lower taxonomic limit of classification with these fingerprints. However, in both cases, the probability of incorrect classification was lower ($\sim$ 83% of cyanobacteria and $\sim$ 76% of Symbiodiniaceae) than the typical classification probabilities of the rest of the endmembers in our study (< 95%). Future studies examining the lower limits of separating these fine scale microalgal fingerprints would greatly improve the field.

Our taxon-specific approach provides new insights into the taxonomic composition of primary producer carbon sources supporting the cauliflower corals through heterotrophy. For example, we determined that picoplankton cells, including prasinophytes (50%) and cyanobacteria (8%), accounted for more than half of the heterotrophically sourced EAA while large celled, diatom-based production accounted for the other 42% (Table S9). Fox et al. (2019) study was conducted at the Palmyra Atoll where strong equatorial upwelling and steep reef slope topography create a high nutrient system that has the potential to support significant diatom production that can be transferred up the food chain to support coral production (Fox et al. 2018). A complementary study using a multitracer fatty acid approach to investigate the trophic strategies of three species of corals in the Maldives, Indian Ocean (Radice et al. 2019) also found that these corals received carbon from a mixed plankton assemblage that included a significant fraction of diatoms. This improved understanding of the carbon sources supporting coral production is important given how critical the balance between autotrophy and heterotrophy is to coral survival and resilience in a changing climate (e.g., Conti-Jerpe et al. 2020).

Conclusions

Our results provide fine-scale taxonomic resolution of $\delta^{13}C_{AAnorm}$ and $\delta^{13}C_{EAAnorm}$ fingerprints of four ecologically important and evolutionarily distinct classes of eukaryotic microalgae. These fingerprints were robust to significant temperature-driven variations in growing conditions and can be applied as tracers of carbon sources supporting upper trophic level consumers. Our ability to diagnostically separate groups of microalgae at the class level will transform our ability to identify changes in microalgal community dynamics spatially and temporally, for example as a function of current and future climate change (Winder and Sommer 2012), and significantly improve the resolution of modern and paleo studies of food web dynamics, biogeochemical cycling, and biological pump dynamics. Future work should aim to expand the taxonomic diversity of this library of eukaryotic microalgal

$\delta^{13}C_{EAAnorm}$ fingerprints to include other underrepresented taxonomic groups in CSIA-AA literature, such as haptophytes and chrysophytes, that are highly abundant, phylogenetically distinct, and ecologically significant microalgal groups in today's oceans. We observed clustering of the replicate cultures of the species within broader taxonomic groups, suggesting perhaps even finer scale resolution of microalgal $\delta^{13}C_{AAnorm}$ fingerprints than the class-level tested in this study. Future work to better understand the isotope effects associated with the diversity of biosynthetic pathways of amino acids among diverse primary producers would greatly improve our ability to develop more predictive models of the separation of taxonomic groups based on their $\delta^{13}C_{AA}$ fingerprints.

Data Availability Statement

All data are archived and openly available through the URI Digital Commons: https://digitalcommons.uri.edu/theses/1936 and NSF BCO-DMO Project 833,411: https://www.bco-dmo.org/project/833411

References

Anderson, S. I., A. D. Barton, S. Clayton, S. Dutkiewicz, and T. A. Rynearson. 2021. Marine phytoplankton functional types exhibit diverse responses to thermal change. Nat. Commun. **12**: 6413. doi:10.1038/s41467-021-26651-8

Arthur, K. E., S. Kelez, T. Larsen, C. A. Choy, and B. N. Popp. 2014. Tracing the biosynthetic source of essential amino acids in marine turtles using $\delta^{13}C$ fingerprints. Ecology **95**: 1285–1293. doi:10.1890/13-0263.1

Barnes, C., D. Maxwell, D. C. Reuman, and S. Jennings. 2010. Global patterns in predator–prey size relationships reveal size dependency of trophic transfer efficiency. Ecology **91**: 222–232. doi:10.1890/08-2061.1

Bartley, T. J., and others. 2019. Food web rewiring in a changing world. Nat. Ecol. Evol. **3**: 345–354. doi:10.1038/s41559-018-0772-3

Besser, A. C., E. A. Elliott Smith, and S. D. Newsome. 2022. Assessing the potential of amino acid $\delta^{13}C$ and $\delta^{15}N$ analysis in terrestrial and freshwater ecosystems. J. Ecol. **110**: 935–950. doi:10.1111/1365-2745.13853

Bianchi, T. S., and E. A. Canuel. 2011. Chemical biomarkers in aquatic ecosystems, p. 30–48. Princeton University Press. doi:10.1515/9781400839100

Binder, S. 2010. Branched-chain amino acid metabolism in *Arabidopsis thaliana*. Arabidopsis Book **8**: e0137. doi:10.1199/tab.0137

Campbell, N. A., J. B. Reese, L. A. Urry, M. L. Cain, S. A. Wasserman, P. V. Minorsky, and R. B. Jackson. 2008. Biology (8th ed). Pearson Benjamin Cummings, San Francisco, CA.

Close, H. G. 2019. Compound-specific isotope geochemistry in the ocean. Ann. Rev. Mar. Sci. **11**: 27–56. doi:10.1146/annurev-marine-121916-063634

Conti-Jerpe, I. E., P. D. Thompson, C. W. M. Wong, N. L. Oliveira, N. N. Duprey, M. A. Moynihan, and D. M. Baker. 2020. Trophic strategy and bleaching resistance in reef-building corals. Sci. Adv. **6**: eaaz5443. doi:10.1126/sciadv.aaz5443

DeNiro, M. J., and S. Epstein. 1977. Mechanism of carbon isotope fractionation associated with lipid synthesis. Science **197**: 261–263. doi:10.1126/science.327

Ducklow, H. W., and others. 2007. Marine pelagic ecosystems: The West Antarctic peninsula. Philos. Trans. R. Soc. B **362**: 67–94. doi:10.1098/rstb.2006.1955

Elliott Smith, E. A., C. Harrod, and S. D. Newsome. 2018. The importance of kelp to an intertidal ecosystem varies by trophic level: Insights from amino acid $\delta^{13}C$ analysis. Ecosphere **9**: e02516. doi:10.1002/ecs2.2516

Elliott Smith, E. A., M. D. Fox, M. L. Fogel, and S. D. Newsome. 2022. Amino acid $\delta^{13}C$ fingerprints of nearshore marine autotrophs are consistent across broad spatiotemporal scales: An intercontinental isotopic dataset and likely biochemical drivers. Func. Ecol. **36**: 1191–1203. doi:10.1111/1365-2435.14017

Falkowski, P. G., E. A. Laws, R. T. Barber, and J. W. Murray. 2003. Phytoplankton and their role in primary, new, and export production, p. 99–121. *In* M. J. R. Fasham [ed.], Ocean biogeochemistry. Springer. doi:10.1007/978-3-642-55844-3_5

Fani, R., and M. Fondi. 2009. The origin and evolution of metabolic pathways. Phys. Life Rev. **6**: 23–52. doi:10.1016/j.plrev.2008.12.003

Ferrier-Pagès, C., M. Hoogenboom, and F. Houlbrèque. 2011. The role of plankton in coral trophodynamics. *In*: Dubinsky, Z., Stambler, N. (eds) Coral Reefs: An Ecosystem in Transition. Springer, Dordrecht. https://doi.org/10.1007/978-94-007-0114-4_15

Field, C. B., M. J. Behrenfeld, J. T. Randerson, and P. Falkowski. 1998. Primary production of the biosphere: Integrating terrestrial and oceanic components. Science **281**: 237–240. doi:10.1126/science.281.5374.237

Fox, M. D., and others. 2018. Gradients in primary production predict trophic strategies of mixotrophic corals across spatial scales. Curr. Biol. **28**: 3355–3363. doi:10.1016/j.cub.2018.08.057

Fox, M. D., E. A. E. Smith, J. E. Smith, and S. D. Newsome. 2019. Trophic plasticity in a common reef-building coral: Insights from $\delta^{13}C$ analysis of essential amino acids. Func. Ecol. **33**: 2203–2214. doi:10.1111/1365-2435.13441

Fry, B., and J. F. Carter. 2019. Stable carbon isotope diagnostics of mammalian metabolism, a high-resolution isotomics approach using amino acid carboxyl groups. PloS One **14**: e0224297. doi:10.1371/journal.pone.0224297

Graham, L. E., J. M. Graham, and L. W. Wilcox. 2009. Algae (2nd ed). Pearson Benjamin Cummings, San Francisco, CA.

Harada, Y., S. Y. Lee, R. M. Connolly, and B. Fry. 2022. Compound-specific isotope analysis of amino acids reveals dependency on grazing rather than detritivory in mangrove food webs. Mar. Ecol. Sci. Proj. **681**: 13–20. doi:10.3354/meps13924

Hayes, J. M. 2001. Fractionation of carbon and hydrogen isotopes in biosynthetic processes. Rev. Mineral. Geochem. **43**: 225–277. doi:10.2138/gsrmg.43.1.225

Jensen, R. A. 1976. Enzyme recruitment in evolution of new function. Ann. Rev. Microbio. **30**: 409–425. doi:10.1146/annurev.mi.30.100176.002205

Kohlmeier, M. 2003. Amino acids and nitrogen compounds, p. 377–383. *In* M. Kohlmeier [ed.], Nutrient metabolism, 2nd ed. Elsevier.

LaJeunesse, T. C., J. E. Parkinson, P. W. Gabrielson, and others. 2018. Systematic revision of Symbiodiniaceae highlights the antiquity and diversity of coral endosymbionts. Curr. Biol. **28**: 2570–2580.

Larsen, T., D. L. Taylor, M. B. Leigh, and D. M. O'Brien. 2009. Stable isotope fingerprinting: A novel method for identifying plant, fungal, or bacterial origins of amino acids. Ecology **90**: 3526–3535. doi:10.1890/08-1695.1

Larsen, T., L. T. Bach, R. Salvatteci, Y. V. Wang, N. Andersen, M. Ventura, and M. D. McCarthy. 2015. Assessing the potential of amino acid ^{13}C patterns as a carbon source tracer in marine sediments: Effects of algal growth conditions and sedimentary diagenesis. Biogeosciences **12**: 4979–4992. doi:10.5194/bg-12-4979-2015

Larsen, T., M. Ventura, N. Andersen, D. M. O'Brien, U. Piatkowski, and M. D. McCarthy. 2013. Tracing carbon sources through aquatic and terrestrial food webs using amino acid stable isotope fingerprinting. PLoS One **8**: e73441. doi:10.1371/journal.pone.0073441

Larsen, T., T. Hansen, and J. Dierking. 2020. Characterizing niche differentiation among marine consumers with amino acid δ^{13}C fingerprinting. Ecol. Evol. **10**: 7768–7782. doi:10.1002/ece3.6502

Lazcano, A., G. E. Fox, and J. F. Orò. 1992. Life before DNA: The origin and evolution of early Archean cells, p. 1–13. *In* R. P. Mortlock and M. A. Gallo [eds.], Experiments in the evolution of catabolic pathways using modern bacteria, the evolution of metabolic functions. CRC Press.

Lehman, J. 2009. Compound-specific amino acid isotopes as tracers of algal central metabolism: Developing new tools for tracing prokaryotic vs. eukaryotic primary production and organic nitrogen in the ocean. M.Sc. thesis. Univ. of California.

Maechler, M., P. Rousseeuw, A. Struyf, M. Hubert, and K. Hornik. 2022. Cluster: Cluster analysis basics and extensions. R package version **2**: 4.

MacDonald, C., T. C. L. Bridge, K. W. McMahon, and G. P. Jones. 2019. Alternative functional strategies and altered carbon pathways facilitate broad depth ranges in coral-obligate reef fishes. Func. Ecol. **33**: 1962–1972. doi:10.1111/1365-2435.13400

Marrec, P., H. McNair, G. Franzè, F. Morison, J. P. Strock, and S. Menden-Deuer. 2021. Seasonal variability in planktonic food web structure and function of the northeast U.S. Shelf. Limnol. Oceanogr. **66**: 1440–1458. doi:10.1002/lno.11696

McMahon, K. W., M. L. Fogel, T. S. Elsdon, and S. R. Thorrold. 2010. Carbon isotope fractionation of amino acids in fish muscle reflects biosynthesis and isotopic routing from dietary protein. J. Anim. Ecol. **79**: 1132–1141. doi:10.1111/j.1365-2656.2010.01722.x

McMahon, K. W., L. L. Hamady, and S. R. Thorrold. 2013. Ocean ecogeochemistry: A review. Oceanogr. Mar. Bio: Ann. Rev. **51**: 327–374.

McMahon, K. W., M. D. McCarthy, O. A. Sherwood, T. Larsen, and T. P. Guilderson. 2015*a*. Millennial-scale plankton regime shifts in the subtropical North Pacific Ocean. Science **350**: 1530–1533. doi:10.1126/science.aaa9942

McMahon, K. W., M. J. Polito, S. Abel, M. D. McCarthy, and S. R. Thorrold. 2015*b*. Carbon and nitrogen isotope fractionation of amino acids in an avian marine predator, the gentoo penguin (*Pygoscelis papua*). Ecol. Evol. **5**: 1278–1290. doi:10.1002/ece3.1437

McMahon, K. W., S. R. Thorrold, L. A. Houghton, and M. L. Berumen. 2016. Tracing carbon flow through coral reef food webs using a compound-specific stable isotope approach. Oecologia **180**: 809–821. doi:10.1007/s00442-015-3475-3

Montes-Hugo, M., S. C. Doney, H. W. Ducklow, W. Fraser, D. Martinson, S. E. Stammerjohn, and O. Schofield. 2009. Recent changes in phytoplankton communities associated with rapid regional climate change along the Western Antarctic peninsula. Science **323**: 1470–1473. doi:10.1126/science.1164533

Newsome, S. D., M. L. Fogel, L. Kelly, and C. M. Rio. 2011. Contributions of direct incorporation from diet and microbial amino acids to protein synthesis in Nile tilapia. Func. Ecol. **25**: 1051–1062. doi:10.1111/j.1365-2435.2011.01866.x

Newsome, S. D., N. Wolf, J. Peters, and M. L. Fogel. 2014. Amino acid δ^{13}C analysis shows flexibility in the routing of dietary protein and lipids to the tissue of an omnivore. Int. Comp. Biol. **54**: 890–902. doi:10.1093/icb/icu106

Not, F., R. Siano, W. H. C. F. Kooistra, N. Simon, D. Vaulot, and I. Probert. 2012. Diversity and ecology of eukaryotic marine phytoplankton. Adv. Bot. Res. **64**: 1–53. doi:10.1016/b978-0-12-391499-6.00001-3

Oksanen, J., and others. 2013. Vegan: Community Ecology Package. R Package Version 2.0-2 **2**: 1–295.

Phillips, N. D., and others. 2020. Bulk tissue and amino acid stable isotope analyses reveal global ontogenetic patterns in ocean sunfish trophic ecology and habitat use. Mar. Ecol. Prog. Ser. **633**: 127–140. doi:10.3354/meps13166

Radice, V. Z., M. T. Brett, B. Fry, M. D. Fox, O. Hoegh-Guldberg, and S. G. Dove. 2019. Evaluating coral trophic strategies using fatty acid composition and indices. PLoS One **14**: e0222327. doi:10.1371/journal.pone.0222327

Rau, G. H., T. Takahashi, and D. J. D. Marais. 1989. Latitudinal variations in plankton δ^{13}C: Implications for CO_2 and productivity in past oceans. Nature **341**: 516–518. doi:10.1038/341516a0

Rau, G., U. Riebesell, and D. Wolf-Gladrow. 1996. A model of photosynthetic ^{13}C fractionation by marine phytoplankton based on diffusive molecular CO_2 uptake. Mar. Ecol. Prog. Ser. **133**: 275–285. doi:10.3354/meps133275

Ros, M., E. F. Camp, D. J. Hughes, J. R. Crosswell, M. E. Warner, W. P. Leggat, and D. J. Suggett. 2020. Unlocking the black-box of inorganic carbon-uptake and utilization strategies among coral endosymbionts (Symbiodiniaceae). Limnol. Oceanogr **65**: 1747–1763. doi:10.1002/lno.11416

Rowe, A. G., K. Iken, A. L. Blanchard, D. M. O'Brien, R. D. Osvik, M. Uradnikova, and M. J. Wooller. 2019. Sources of primary production to Arctic bivalves identified using amino acid stable carbon isotope fingerprinting. Isotopes Environ. Health Stud. **55**: 1–19. doi:10.1080/10256016.2019.1620742

Scott, J. H., D. M. O'Brien, D. Emerson, H. Sun, G. D. McDonald, A. Salgado, and M. L. Fogel. 2006. An examination of the carbon isotope effects associated with amino acid biosynthesis. Astrobiology **6**: 867–880. doi:10.1089/ast.2006.6.867

Shen, Y., T. P. Guilderson, O. A. Sherwood, C. G. Castro, F. P. Chavez, and M. D. McCarthy. 2021. Amino acid $\delta^{13}C$ and $\delta^{15}N$ patterns from sediment trap time series and deep-sea corals: Implications for biogeochemical and ecological reconstructions in paleoarchives. Geochim. Cosmochim. Acta **297**: 288–307. doi:10.1016/j.gca.2020.12.012

Sieburth, J., V. Smetacek, and J. Lenz. 1978. Pelagic ecosystem structure: Heterotrophic compartments of the plankton and their relationship to plankton size fractions. Limnol. Oceanogr. **23**: 1256–1263. doi:10.4319/lo.1978.23.6.1256

Silfer, J. A., M. H. Engel, S. A. Macko, and E. J. Jumeau. 1991. Stable carbon isotope analysis of amino acid enantiomers by conventional isotope ratio mass spectrometry and combined gas chromatography/isotope ratio mass spectrometry. Anal. Chem. **63**: 370–374.

Skinner, C., A. C. Mill, M. D. Fox, S. P. Newman, Y. Zhu, A. Kuhl, and N. V. C. Polunnin. 2021. Offshore pelagic subsidies dominate carbon inputs to coral reef predators. Sci. Adv. **7**: eabf3792. doi:10.1126/sciadv.abf3792

Sorochan, K. A., S. Plourde, R. Morse, P. Pepin, J. Runge, C. Thompson, and C. L. Johnson. 2019. North Atlantic right whale (*Eubalaena glacialis*) and its food: (II) interannual variations in biomass of *Calanus spp.* on western North Atlantic shelves. J. Plankton Res. **41**: 687–708. doi:10.1093/plankt/fbz044

Stamieszkin, K., A. J. Pershing, N. R. Record, C. H. Pilskaln, H. G. Dam, and L. R. Feinberg. 2015. Size as the master trait in modeled copepod fecal pellet carbon flux. Limnol. Oceanogr. **60**: 2090–2107. doi:10.1002/lno.10156

Takizawa, Y., Y. Takano, B. Choi, P. S. Dharampal, S. A. Steffan, N. O. Ogawa, N. Ohkouchi, and Y. Chikaraishi. 2020. A new insight into isotopic fractionation associated with decarboxylation in organisms: Implications for amino acid isotope approaches in biogeoscience. Prog Earth Planet Sci **7**: 1–13. doi:10.1186/s40645-020-00364-w

Tirichine, L., and C. Bowler. 2011. Decoding algal genomes: Tracing back the history of photosynthetic life on earth. Plant J. **66**: 45–57. doi:10.1111/j.1365-313x.2011.04540.x

Venables, W. N., and B. D. Ripley. 2002. Modern applied statistics with S, 4th ed. Springer.

Vokhshoori, N., T. Larsen, and M. McCarthy. 2014. Reconstructing $\delta^{13}C$ isoscapes of phytoplankton production in a coastal upwelling system with amino acid isotope values of littoral mussels. Mar. Ecol. Prog. Sci. **504**: 59–72. doi:10.3354/meps10746

Wall, C. B., N. J. Wallsgrove, R. D. Gates, and B. N. Popp. 2021. Amino acid $\delta^{13}C$ and $\delta^{15}N$ analyses reveal distinct species-specific patterns of trophic plasticity in a marine symbiosis. Limnol. Oceanogr. **66**: 2033–2050. doi:10.1002/lno.11742

Ward, C. L., and K. S. McCann. 2017. A mechanistic theory for aquatic food chain length. Nat. Commun. **8**: 2028. doi:10.1038/s41467-017-02157-0

Whiteman, J. P., S. L. Kim, K. W. McMahon, P. L. Koch, and S. D. Newsome. 2018. Amino acid isotope discrimination factors for a carnivore: Physiological insights from leopard sharks and their diet. Oecologia **188**: 977–989. doi:10.1007/s00442-018-4276-2

Winder, M., and U. Sommer. 2012. Phytoplankton response to a changing climate. Hydrobiologia **698**: 5–16. doi:10.1007/s10750-012-1149-2

Yarnes, C. T., and J. Herszage. 2017. The relative influence of derivatization and normalization procedures on the compound-specific stable isotope analysis of nitrogen in amino acids. Rapid Commun. Mass. Spec. **31**: 693–704. doi:10.1002/rcm.7832

Ycas, M. 1974. On earlier states of the biochemical system. J. Theor. Biol. **44**: 145–160. doi:10.1016/S0022-5193(74)80035-4

Acknowledgments

We thank Drs. C. Thornber, B. Govenar, S. Menden-Deuer, T. Larsen, and O. Sherwood for discussions on experimental design and data interpretation. M. McKenzie, A. Montalbano, E. Rubin, J. Carney, S. Setta, I. Bishop, and D. Outram for microalgae culturing and equipment assistance. J. Langan for statistical assistance, and R. Patrick Kelly for mass spectrometry assistance. This work was funded through the Rhode Island Science and Technology Advisory Council (KWM: 06561) and the National Science Foundation (KWM: 1826712, 2049307).

Conflict of Interest

None declared

Submitted 14 July 2022
Revised 23 November 2022
Accepted 16 March 2023

Associate editor: C. Elisa Schaum